ANALYSIS OF MAGNETIC FEATURES IN IPMSM USED FOR EV CONSIDERING PM - FLUX BARRIER INTERACTION AND EXCITATION CURRENT

PHÂN TÍCH TÍNH CHẤT TỪ TRONG ĐỘNG CƠ ĐỒNG BỘ IPM DÙNG CHO XE ĐIỆN XEM XÉT ĐẾN SỰ TƯƠNG TÁC NAM CHÂM – RÀO CHẮN TỪ THÔNG VÀ DÒNG ĐIỆN LÀM VIỆC

Ho Quang Viet[1], Duc-Kien Ngo[1]*, Nguyen Vu Thanh[2], Anh Tuan Phung[2], Ngo Huy Dong[2], Le Cong Han[1], Doan Van Khanh[1]

[1]The University of Danang - University of Technology and Education
[2]Hanoi University of Science and Technology

*Corresponding author: ndkien@ute.udn.vn

(Received: September 15, 2023; Revised: November 18, 2023; Accepted: November 21, 2023)

Abstract - This paper analysis the magnetic features including flux linkage and air-gap flux density in interior permanent magnet synchronous motor (IPMSM) with delta-shaped PM used for electric vehicles (EVs). Research motor models are based on the motor of Nissan Leaf called EM61 taken from experiment reports, and the analysis is based on finite element analysis (FEA). The analysis is performed by adjusting the existence of permanent magnets (PMs) and flux barriers (FBs) as well as the amplitude and phase angle of excitation current which affect the torque production, phase flux linkage, and air-gap flux density under two temperature conditions. Through this analysis, the influence of each object, its position (i.e., the inner and outer layer of PM and FB), and PM-FB interaction on the magnetic features of IPMSM are expressed. The role of these PM-FBs on magnetic features also helps to point out some indications for engineers when designing an IPMSM.

Key words - Interior permanent magnet synchronous motor (IPMSM); delta-shaped PM; phase flux linkage; air-gap flux density

Tóm tắt - Bài báo phân tích các tính chất từ gồm từ thông móc vòng và mật độ từ thông khe hở không khí trong động cơ đồng bộ nam châm vĩnh cửu gắn chìm (IPMSM) với nam châm vĩnh cửu (NCVC hay PM) xếp tam giác dùng cho xe điện (EVs). Các mẫu nghiên cứu dựa trên động cơ EM61 của Nissan Leaf từ các báo cáo thử nghiệm và việc phân tích dựa trên phân tích phần tử hữu hạn (FEA). Nghiên cứu điều chỉnh sự tồn tại của NCVC và rào chắn từ thông (FB) cũng như biên độ và góc pha của dòng điện làm việc làm ảnh hưởng đến việc sản sinh mô-men, từ thông móc vòng pha và mật độ từ thông khe hở không khí trong hai điều kiện nhiệt độ. Qua đó ảnh hưởng của từng đối tượng, vị trí (lớp bên trong và bên ngoài của PM và FB) và sự tương tác của PM-FB đến các tính chất từ của IPMSM được thể hiện. Vai trò của các PM-FB đối với các đặc điểm từ tính cũng giúp chỉ ra một số chỉ dẫu cho các kỹ sư khi thiết kế.

Từ khóa - Động cơ đồng bộ nam châm vĩnh cửu gắn chìm; nam châm vĩnh cửu xếp hình tam giác; từ thông móc vòng pha; mật độ từ thông khe hở không khí.

1. Introduction

Recently, electric vehicles (EVs) have been one of the hot topics in the world where electric motors used for EVs are of great interest to electrical engineers. Interior permanent magnet synchronous motor (IPMSM) is considered the top choice for this application [1] since its merits consist of high torque density, high efficiency, and wide operating speed range, etc [2]–[5]. There are many IPMSM models that are being considered for introduction to EVs which can be listed as V-shaped [3], delta-shaped [6], Y-shaped [7], etc., and so on a number of studies compare IPMSM and other EV motor candidates. Liu et al. investigated the performances and parameters of four IPMSM models consisting of spoke-type, tangential-type, U-shaped, and V-shaped. Performance analysis of V-shaped based on the 2004 Toyota Prius's IPM, spoke-type IPM, and the induction motor (IM) for hybrid vehicles is presented in [8]. The high-performance fractional slot concentrated winding IPMSMs including Y-shaped, V-shaped, and Spoke-type are compared and proposed by Dutta et al. [7]. Yang et al. presented the design and performance comparison between three motors including Delta-shaped, Double V-shaped, and Single V-shaped where the Delta-shaped one referred to the motor of Nissan Leaf [9]. On the other hand, a series of experiment reports of practice motors for EVs including Toyota Prius, Nissan Leaf, Hyundai Sonata, etc., which is performed to provide comprehensive technical information [10]–[13]. However, these studies hardly analyze the problems of each permanent magnet-flux barrier (PM-FB) layer and the changing of excitation.

This paper approaches directly the rotor configuration of IPMSM to consider not only the interaction between PM and FB but also the excitation current to characteristics of the magnetic field. For this purpose, we chose the motor called EM61 used for Nissan Leaf with the delta-shaped conducted, and the motor's design data are taken from the experiment reports of EV motors [10]–[13]. We focus on the trend of phase flux linkage and air-gap flux density which is closely related to torque production when PM-FB layers as well as only PM or FB are eliminated under the condition that the amplitude and phase angle of excitation current are adjusted. From these analyses, the role of PM, FB, PM-FB interaction, and excitation current on magnetic features of IPMSM are clarified. To accommodate actual resources, the study will be based on finite element analysis

(FEA) with great care in setting up, collecting, reporting, and evaluating results.

2. Background of wide speed range motors, mathematical and investigated models

2.1. Theory of motor with wide speed range

Different from electric motors used in common industrial devices, electric motors used for EVs need a wide operating speed range to coincide with the operating characteristics of the vehicle. The basic operation characteristics of the EV motor are shown in Figure 1 where three regions are approached and operated. The first region is on the left hand of the speed range where the speed is low while torque is very high. This region is the current-limited region and could be called maximum torque per ampere (MTPA) meaning the amplitude of excitation current is fixed at a based value while the current angle is selected so that the maximum torque can be achieved. Note that the voltage will increase with speed in this region. For urban EV motors, the top speed of this region, or could be called the based speed is about several thousand revolutions per minute (rpm). Next to the right of the MTPA region is the current-and-voltage-limited region meaning when the voltage meets the limited value of power supply while the current amplitude is continuously fixed to the based value. However, the current phase angle needs to be changed depending on speed. The last region is the voltage-limited region and could be called maximum torque per voltage (MTPV) meaning current amplitude and phase angle are controlled to get maximum torque when voltage is limited by drive. Two latter regions can be collectively referred to as field weakening operations where the torque must be reduced when speed increases, through proactive weakening of the magnetic flux of the motor by adjusting the excitation current.

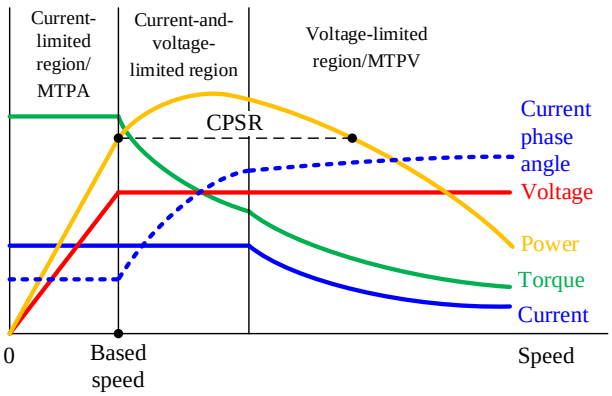

Figure 1. *Basic electrical and mechanical characteristics of the motor*

In terms of output power vs. speed, field weakening operation is limited by two speed values, the first is the top speed of the MTPA region or base speed (point F) and the second (point S) is the speed where its output power is equal to the output power according to the base speed. The ratio of these two-speed values is called the constant power speed ratio (CPSR), where the CPSR of an EV motor should probably be greater than three or four so that the top speed of the EV motor could be tens of thousands of rpm.

Based on the theory of EV motors and the popularity of PMSM in this application, the current is manipulated to weaken the magnetic flux which helps to increase motor speed over base one. This means the magnetic issue in PMSM is affected by two magnetic sources, the excitation current and PM. In addition, the existence of flux barriers (FBs) to place the PM will also have an impact on the distribution and characteristics of the magnetic field and motor performance.

2.2. Mathematical and investigated models

For IPMSM, the voltage and torque equations are described below,

$$V = \omega\sqrt{\left(-L_d I_d + \lambda_m\right)^2 + \left(L_q I_q\right)^2} \tag{1}$$

$$T = \frac{3}{2} p\left[\lambda_m I_q + \left(L_d - L_q\right) I_d I_q\right] \tag{2}$$

$$\lambda_d = -L_d I_d + \lambda_m,\ \lambda_q = L_q I_q \tag{3}$$

$$\lambda_d = -L_d I_d + \lambda_m,\ \lambda_q = L_q I_q \tag{4}$$

where subscripts d and q represent d- and q-axis, respectively, I_d and I_q are the currents, λ_d and λ_q are the flux linkages, λ_m is magnet flux linkage, and ω is the electrical angular speed.

Note that, the flux d- and q- flux linkages, inductances, and currents are respectively transformed from the phase flux linkages, inductance, and currents. In other words, the magnetic parameters are transformed from the stator reference frame (i.e., *abc* frame) to the rotor reference frame (i.e., *dq* frame) [14]. In addition, as their name suggests, FBs hinder the flux leading to the changing of reluctances or inductances of the motor which influences motor performance. For another type of motor with embedded PM called PM-assisted synchronous reluctance motor (PMa-SynRM), the FBs play a dominant role in motor performance [15], [16], so the design theory is proposed [17]. However, for IPMSM, the role of FBs is often understood as places where PMs are located. This paper therefore examines FB in relation to PM (i.e., PM-FB interaction) where the analysis and interpretation will be presented in the next section.

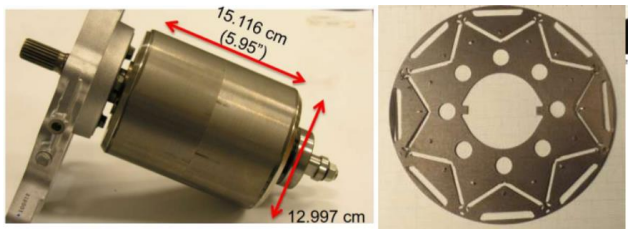

Figure 2. *Practice motor EM61 was used for the Nissan Leaf 2012 [18]*

The analyzed IPMSM models are based on the practice motor used for Nissan Leaf 2012 called EM61 where the delta-shaped PM is conducted in the rotor [18] as shown in Figure 2. The delta-shaped PM rotor consists of two PM and flux barrier layers, the outer one near to air-gap is only one PM piece (Out. PM) with a parallel flux pattern that is perpendicular to the radius, and the inter one is a pair of

symmetrical PMs forms a V shape (Left and Right Int. PMs) and also has parallel flux pattern that is perpendicular to its wide side. The detail rotor and *d*-*q* coordinate are illustrated in Figure 3, where the *d*-axis is assigned the main direction of PMs, i.e., parallel to the flux pattern of outer PM, and the current phase angle is advanced from the *d*-axis to the *q*-axis.

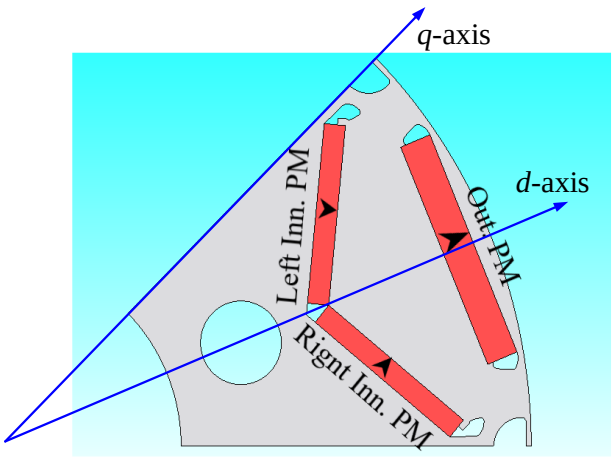

Figure 3. *The rotor construction of EM61 and d-q coordinate. Note that the d-axis is the reference for the current phase angle*

For such a practice motor, the design construction is predetermined including PM and FB sizes, FB angle, rotor rib, etc., which will intentionally not be considered according to the initial goals of this paper. To assess PM-FB interaction on the magnetic issue of the motor, the PM-FB or only PM will be removed from the original model leading to other models which are clearly introduced in Table 1. In addition, the material information and winding configuration of the motor are described in Table 2 and Figure 4.

Table 1. *List of investigated models*

No.	Model	Description
1	Origin	The initial rotor
2	Inn.PMs	All the outer PM and FB are removed
3	Inn.PMs-OutPM	The outer PM is removed and the outer FB is kept
4	Out.PM	All inner PMs and FBs are removed
5	Out.PM-Inn.FBs	The inner PMs are removed and the inner FBs are kept

Table 2. *Material, winding configuration, and PM area per pole of motors*

No.	Items	Value
1	Material of stator and rotor cores	30 DH
2	Material of PM	N30UH
3	Number of slots	48
4	Number of pole pairs	4
5	Number of winding layers	1
6	Coil pitch	5
7	Number of turns	6
8	Area of outer PM per pole	107.4 mm^2
9	Area of inner PMs per pole	110.9 mm^2

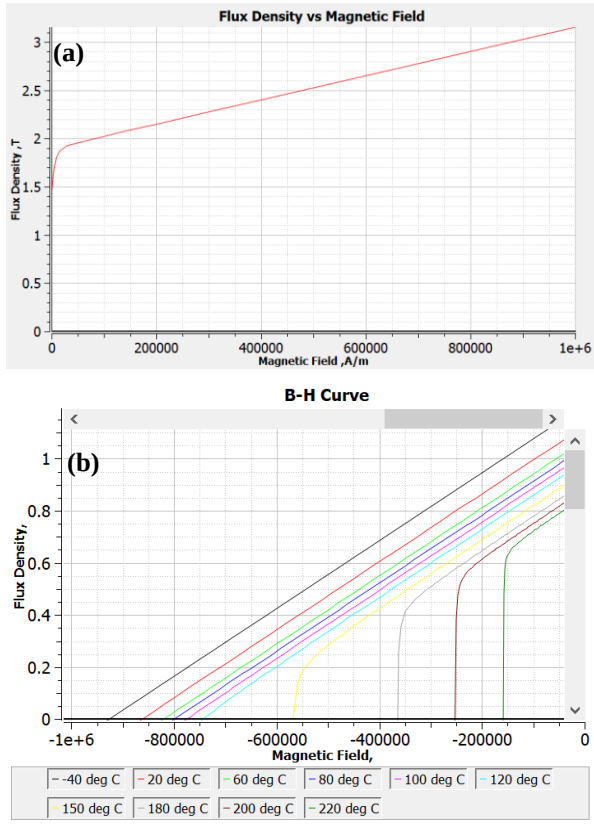

Figure 4. *B-H curve of materials. (a) 30 DH. (b) N30UH. Note that the illustrations are extracted from the software environment*

Different from many papers where the comparisons are made across different types of model structures, the investigated models in this paper are based on only one motor where parts of the rotor structure (i.e., PM or FB) are removed. This means when a PM is removed, the flux source will be reduced, whereas when a FB is removed, the path of flux will be changed, leading to changes in the magnetic features including flux linkage and air-gap flux density. This will be directly related to differences in torque production which will be presented in the next section.

3. Motor performance analysis

3.1. Torque production and magnetic features at based current

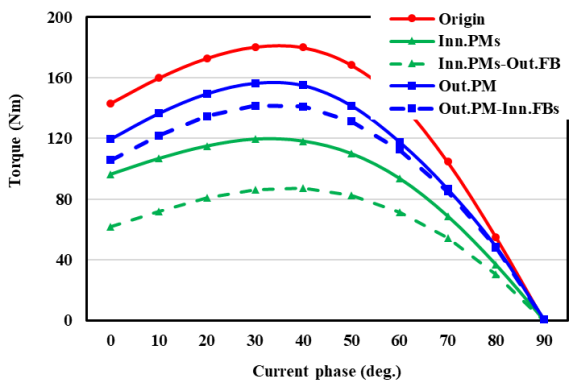

Figure 5. *Torque production comparison*

The torque production of five models named in Table 1 is investigated where the based current, i.e., 280 A peak is

applied and the current phase angle is changed from 0 to 90 degrees. This comparison is shown in Figure 5. It can be seen that the maximum torque of these models is achieved at approximately the same current phase angle (i.e., around 35 degrees) as presented in Table 3, while these values are quite different. Some problems can be discussed following.

Table 3. *Maximum torque and current angle values at 280 A peak of excitation current*

No.	Model	Current angle (degree)	Maximum torque (Nm)	Lower percent (%)
1	Origin	35	181.6	0.0
2	Inn.PMs	33	120.0	33.9
3	Inn.PMs-Out.PM	37	87.6	51.8
4	Out.PM	34	157.0	13.5
5	Out.PM-Inn.FBs	34	142.3	21.7

Firstly, the torque is decreased when removing PM, and removing outer PM (i.e., Inn.PMs model) results in much more severe degradation than removing the inner PM (i.e., Out.PM model), namely 33.9 % versus 13.4 %. The degradation of torque production can be simply explained by the decrease in the amount of magnetic flux that is supplied by the PMs. Further clarification can be achieved through consideration of phase flux linkages at the no-load condition as shown in Figure 6, when these phase flux linkages are attended by only PM flux. As can be seen in Figure 6(a), although the amplitudes are not significantly different, the phase flux linkage at no-load of the Out.PM model is wider than that of the Inn.PMs model. As a result, the fundamental component of phase flux linkage of the Out.PM model is higher than that of the Inn.PMs model, which is shown in Figure 6(b). In addition, the fundamental component can essentially represent the phase flux linkage level in this study.

Secondly, a quite interesting thing is that if we only remove the PMs but keep the existing FBs (i.e., Inn.PMs-Out.PM and Out.PM-Inn.FBs models), the torque production decreases even more, 51.8 % vs 33.5 % and 21.7 % vs 13.5 %, respectively. This may seem counterintuitive when compared with the theory of permanent magnet-assisted synchronous reluctance motor (PMa-SynRM) where the more FBs the more saliency the more torque production [19]. This can be explained by the fact that for PMSM, the FBs are mainly responsible for having room to place the PM in the rotor structure. Improper arrangement of FBs even hinders magnetic flux, leading to affecting torque production.

Finally, according to the change of torque production vs. current phase angle, the fundamental component of the phase flux linkage is also changed when the phase angle of excitation changes from 0 to 90 degrees, as can be seen in Figure 7. However, different from torques that achieve their maximum values at around 35 degrees of the current phase angle, the fundamental components of the phase flux linkage of all models gradually deteriorate from the maximum values at 0 degrees to around 35 degrees where the torque is maximum (the drop percent are about 10 to 17). Note that the 0 degrees of the current phase angle correspond to magnetic flux based on excitation current is parallel to PM flux. These imply the torque production in PMSM is not only based on the interaction between PM flux and excitation current (i.e., PM torque) but also based on the saliency by the exciting of FBs (i.e., reluctance torque) [19]. In addition, the phase flux linkages are dramatically dropped over that current phase angle.

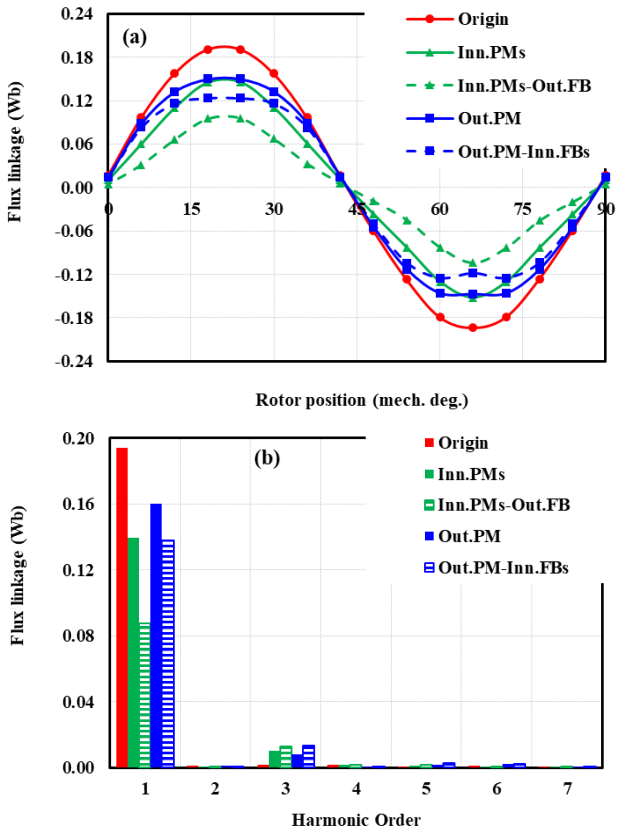

Figure 6. *Comparison of flux linkage and harmonic components at no-load. (a) Flux linkages. (b) Harmonic amplitudes*

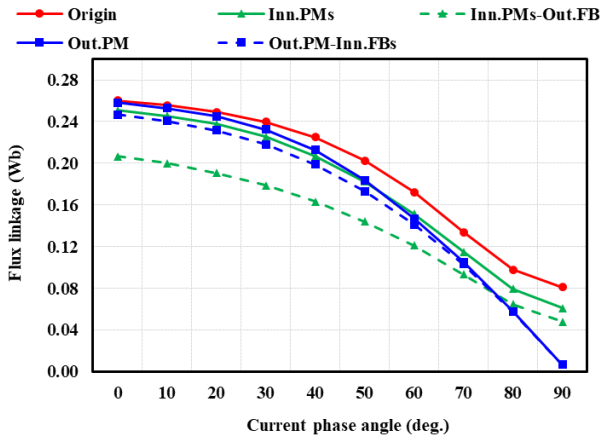

Figure 7. *Fundamental component of phase flux linkage vs. current phase angle*

3.2. Effect of amplitude and phase angle of current to magnetic features

As analyzed above, the current phase angle will affect

the magnetic features of the motor, so in this section, we will focus on evaluating the influence of the amplitude and phase angle of current according to the position of the magnet without changing the stator core structure. More specifically, we will first change the current amplitude for the Origin model, then change the current angle and remove specific PM from the existing rotor structure. In addition, we consider both phase flux linkage and air-gap flux density.

3.2.1. Effect of current amplitude

The amplitude of the excitation current is adjusted from 80 to 280 A in 50 A tuning steps while the current phase angle is fixed at 0 degrees for only the Origin model. This is to assess the highest magnetic features for the practice motor. The comparison of fundamental components of phase flux linkage and rms of air-gap flux density is shown in Figure 8. As can be seen, the lower the current amplitude, the lower the fundamental components of phase flux linkage and air-gap flux density. Besides, when the PM temperature increases (i.e., 150ºC), both of the fundamental components of phase flux linkage and air-gap flux density are dropped. This is because, at the high temperature, the magnetism capacity of PM will be decreased as shown in Figure 4. It should be noted that these declines in magnetic features will be related to the ability of torque production and motor efficiency.

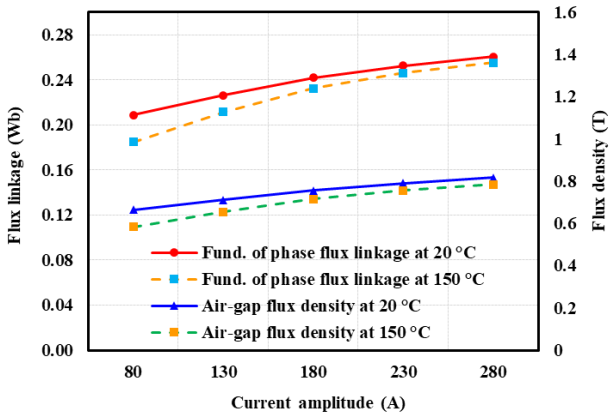

Figure 8. *Fundamental component of phase flux linkage and rms of air-gap flux density vs. current amplitude for Origin model*

3.2.2. Effect of current phase angle

Since the fundamental components of phase flux linkage of the five models are investigated in the upper section, only the investigation of air-gap flux density is conducted here. Besides, the rotor core structure including FBs is maintained, and only one PM layer is placed, i.e., Inn.PMs-Out.PM and Out.PM-Inn.FBs are used for the purpose of assessing the role of PM. Figure 9 shows the effect of current phase angle at based current (i.e., 280 A of amplitude) on air-gap flux density. It can be seen, similar to phase flux linkages which are illustrated in Figure 7, that the rms of air-gap flux densities decline when the current phase angle changes from 0 to 90 degrees. However, the decline of phase flux linkage and air-gap flux density here and also in Section 3.2.1 could not be serious problems because these are consistent with the theory of wide speed range of motor as presented in Section 2.1.

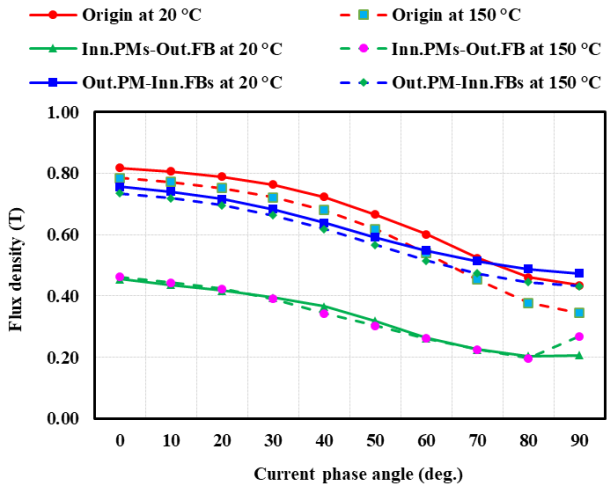

Figure 9. *RMS of air-gap flux density vs. current phase angle*

Besides, the rms of air-gap flux density of Out.PM-Inn.FBs model is slightly lower than that of the Origin model while that of Inn.PMs-Out.FB is extremely low compared to others. It can be observed that because the PM of Out.PM model is close to the air-gap so that the air-gap flux density is higher. These imply the outer PM plays a much more important role than inner PMs in the magnetic features of this motor. However, the existence of inner PMs will also yield some improvement in the magnetic features which is realized in terms of an increase in torque production as presented in Section 3.1.

4. Conclusions

In this paper, the magnetic features of a delta-shaped IPMSM used for EV are analyzed. The PMs and FBs are intentionally set to evaluate the interaction between them and to magnetic features of motor. Besides, the torque production, phase flux linkage, and air-gap flux density were investigated when the amplitude and phase angle of the excitation current were adjusted. These analyses found that the outer PM plays a key role in shaping magnetic features and torque production while the inner PMs have a complementary and improving role. Meanwhile, FBs mainly are rooms to place PM, which even reduces the magnetic features of motor if there is the disappearance of PMs. On the other hand, low amplitude and high phase angle of excitation current will attenuate phase flux linkage and air-gap flux density. The indications of the role of PM-FB in this paper can also be helpful to engineers when designing an IPMSM. In addition, the whole design parameters such as PM and FB sizes, FB angle, rotor rib, etc., will be evaluated in future design studies.

Acknowledgment: This research is funded by Funds for Science and Technology Development of the University of Danang under project number B2022-DN06-03. The authors would like to thank Prof. Min-Fu Hsieh and Prof. Nguyen Gia Minh Thao for supporting research resources.

REFERENCES

[1] Z. Wang, T. W. Ching, S. Huang, H. Wang, and T. Xu, "Challenges Faced by Electric Vehicle Motors and Their Solutions", *IEEE Access*, vol. 9(1), pp. 5228–5249, 2021, doi: 10.1109/ACCESS.2020.3045716.

[2] N. Bianchi and S. Bolognani, "Interior PM synchronous motor for high performance applications", in *Proceedings of the Power Conversion Conference-Osaka 2002 (Cat. No.02TH8579)*, IEEE, 2002, pp. 148–153. doi: 10.1109/PCC.2002.998538.

[3] Y. Kong, M. Lin, and L. Jia, "A Novel High Power Density Permanent-Magnet Synchronous Machine With Wide Speed Range", *IEEE Trans Magn*, vol. 56, no. 2, pp. 1–6, Feb. 2020, doi: 10.1109/TMAG.2019.2947611.

[4] S.-I. Kim, Y.-K. Kim, G.-H. Lee, and J.-P. Hong, "A Novel Rotor Configuration and Experimental Verification of Interior PM Synchronous Motor for High-Speed Applications", *IEEE Trans Magn*, vol. 48, no. 2, pp. 843–846, Feb. 2012, doi: 10.1109/TMAG.2011.2174045.

[5] X. Zhu, W. Wu, L. Quan, Z. Xiang, and W. Gu, "Design and Multi-Objective Stratified Optimization of a Less-Rare-Earth Hybrid Permanent Magnets Motor With High Torque Density and Low Cost", *IEEE Transactions on Energy Conversion*, vol. 34, no. 3, pp. 1178–1189, Sep. 2019, doi: 10.1109/TEC.2018.2886316.

[6] T. Song, Z. Zhang, H. Liu, and W. Hu, "Multi-objective optimisation design and performance comparison of permanent magnet synchronous motor for EVs based on FEA", *IET Electr Power Appl*, vol. 13, no. 8, pp. 1157–1166, Aug. 2019, doi: 10.1049/iet-epa.2019.0069.

[7] R. Dutta, A. Pouramin, and M. F. Rahman, "A Novel Rotor Topology for High-Performance Fractional Slot Concentrated Winding Interior Permanent Magnet Machine", *IEEE Transactions on Energy Conversion*, vol. 36, no. 2, pp. 658–670, Jun. 2021, doi: 10.1109/TEC.2020.3030302.

[8] D. G. Dorrell, A. M. Knight, L. Evans, and M. Popescu, "Analysis and Design Techniques Applied to Hybrid Vehicle Drive Machines - Assessment of Alternative IPM and Induction Motor Topologies", *IEEE Transactions on Industrial Electronics*, vol. 59, no. 10, pp. 3690–3699, Oct. 2012, doi: 10.1109/TIE.2011.2165460.

[9] Y. Yang *et al.*, "Design and Comparison of Interior Permanent Magnet Motor Topologies for Traction Applications", *IEEE Transactions on Transportation Electrification*, vol. 3, no. 1, pp. 86–97, Mar. 2017, doi: 10.1109/TTE.2016.2614972.

[10] S. A. Rogers, *Annual Progress Report for the Advanced Power Electronics and Electric Motors Program*. US Department of Energy, 2013.

[11] J. M. Miller, *Electric Motor R&D*. Oak Ridge National Laboratory, 2013.

[12] T. Burress, *Benchmarking State-of-the-Art Technologies*. Oak Ridge National Laboratory, 2013.

[13] T. Burress, *Benchmarking of Competitive Technologies*. Oak Ridge National Laboratory, 2012.

[14] R. E. Neapolitan and K. H. Nam, *AC Motor Control and Electrical Vehicle Applications*. CRC Press, 2018. doi: 10.1201/9781315200149.

[15] Ngo and Hsieh, "Performance Analysis of Synchronous Reluctance Motor with Limited Amount of Permanent Magnet", *Energies (Basel)*, vol. 12, no. 18, p. 3504, Sep. 2019, doi: 10.3390/en12183504.

[16] M. S. Mirazimi and A. Kiyoumarsi, "Magnetic Field Analysis of SynRel and PMASynRel Machines with Hyperbolic Flux Barriers Using Conformal Mapping", *IEEE Transactions on Transportation Electrification*, vol. 6, no. 1, 2020, doi: 10.1109/TTE.2019.2959400.

[17] N. Bianchi, H. Mahmoud, S. Bolognani, H. Mahmoud, and N. Bianchi, "Fast synthesis of permanent magnet assisted synchronous reluctance motors", *IET Electr Power Appl*, vol. 10, no. 5, pp. 312–318, May 2016, doi: 10.1049/iet-epa.2015.0240.

[18] D. Staton and J. Goss, *Open Source Electric Motor Models for Commercial EV & Hybrid Traction Motors*. CWIEME 2017, 2017.

[19] R. Vartanian and H. A. Toliyat, "Design and comparison of an optimized permanent magnet-assisted synchronous reluctance motor (PMa-SynRM) with an induction motor with identical NEMA Frame stators", in *2009 IEEE Electric Ship Technologies Symposium*, IEEE, Apr. 2009, pp. 107–112. doi: 10.1109/ESTS.2009.4906501.